Pol. J. Environ. Stud. Vol. 24, No. 3 (2015), 1309-1316

Original Research

Corrosion of Hardened Cement Paste in Concrete used for Building Coke Wastewater Treatment Plant Tanks

Barbara Słomka-Słupik*, Adam Zybura

Faculty of Civil Engineering, Silesian University of Technology
Akademicka 5, 44-100 Gliwice, Poland

Received: 9 November 2013
Accepted: 12 December 2014

Abstract

This work pays attention to the possibility of formation leakage through reinforced concrete walls of sewage tanks. Leakage can be caused by the action of aggressive components of wastewater on concrete. Hardened cement paste can be damaged by chloride and ammonium ions present in significant quantities in the post-production waters from coking plants. This important kind of concrete corrosion was precisely recognized in laboratory conditions. Specimens of cement pastes made from two different cements were immersed in saturated water solutions of ammonium chloride. The test results of porosity, chloride ion concentrations, and content of crystal phases showed large changes in the microstructure of hardened cement pastes. We found that the Portland cement used in the postwar years provide better durability than the slag cement currently recommended for constructing environmental protection facilities.

Keywords: corrosion, ammonium chloride, decalcification, coke sewage

Introduction

Reinforced concrete tanks for liquid wastewater storage should provide a solid barrier, protecting the natural environment. However, damage to the walls of these objects in many in-plant wastewater treatment plants has been reported. The problem is that sewage tanks are, in most cases, recessed in the ground so that environmental contamination by leaking walls cannot be noticed in the long term. This problem mainly affects industrial wastewater treatment plants, where concentrations of pollutants are generally higher than in municipal sewage. These waters in their composition contain substances: hazardous, toxic, and carcinogenic – to health and life, as well as ions – unfavorably acting on reinforced concrete. Therefore, this work focuses on concrete corrosion of the tanks of coke sewage treatment plants. Coke plants are located mainly in Poland's Silesia region.

So far, no attention has been paid to leakage of wastewater objects caused by concrete corrosion. The phenomenon occurring in the concrete under the influence of ammonium chloride was also not studied in a precise manner. So the aim of this study was comparison of the features determining durability of hardened pastes made from two different cements used for construction of sewage treatment plant objects. The changes of microstructure (as porosity), content of chloride ions, and the presence of crystalline phases along the way of diffusion of aggressive ions were analyzed. Our examination focused on cement paste – the component most vulnerable to corrosion.

*e-mail: Barbara.Slomka-Slupik@polsl.pl

Aggressiveness of Coke Wastewater in Relation to Cement Paste

Hardened concrete, from which walls of sewage facilities are constructed, consists of a hardened cement paste and mineral aggregate, in some cases chemical admixtures and additives as well. It is porous material that can easily be penetrated by substances from the external environment. The most vulnerable to aggressive influences is binder: hydrated cement paste composed of calcium silicate hydrate (called C-S-H phase), involved in about 2/3 of the volume; portlandite $Ca(OH)_2$ (by nomenclature: C-H), constituting about 20% of the volume; and calcium aluminate hydrates – about 10% of the volume; and other phases in lower amounts. Pores occupy around 20% of the volume of hardened cement paste [1]. Moisture present in the cement paste is characterized by highly alkaline (pH ≈ 13) reactivity. This value of pH ensures proper protection from corrosion to reinforcement steel. Reduction in pH causes a disturbance of thermodynamic equilibrium between phases of hydrated cement paste and solution present in pores. Such destructive action of concrete causes coke wastewaters. They are characterized by pH = 8 [1-6]. Aggressiveness of waste water is increased by ammonium and chloride ions contributing to reduce the pH even to 6. Chloride ions in coke wastewater achieve a concentration of 1280-5800 g Cl^-/m^3, while the ammonium ions achieve a concentration of 127-4122 g $N\text{-}NH_3/m^3$ (maximum 8700 g $N\text{-}NH_3/m^3$) [6-8].

The mechanism of cement paste destruction is characterized by ion exchange. Cl^- ions diffused into the concrete are placed by OH^- ions, according the principle of balancing the negative charges. Therefore, the content of OH^- ions decreases toward the external surface of the concrete, which is in contact with the solution [9]. Chloride ions are highly mobile, so the exchange reactions $Cl^- \rightarrow OH^-$ are rapid. Diffusing chlorides cause the corrosion of reinforcement steel and contribute indirectly to decalcification of hardened cement paste. They react with Ca^{2+} ions to form $CaCl_2$, which is easily soluble in water. As a result of dissolution, the calcium ions are diffusing toward the concrete external surface. Chloride ions cause binding the Ca^{2+} ions into more complex chloride solid phases, as well as [1, 10-12]. Chlorides contained in the hardened cement paste exist in free (diffusing Cl^- ions) and in bound forms. Between those two forms of chloride ions an equilibrium is established. This equilibrium can be disturbed by the changes of the pore solution composition [1, 13]. As previously mentioned, Cl^- ions can form different crystalline phases in the hardened cement paste. The most likely is the formation of Friedel's salt $C_3A{\cdot}CaCl_2{\cdot}10H_2O$. This is considered to be beneficial because of the reduction the free Cl^- ions in pore solution. During chloride aggression it may also be achieved, creating non-chloride sulphate phases – expansive ettringite and thaumasite. Thaumasite is not a biding phase, so its formation weakens the cement matrix [1, 5, 14, 15].

Ammonium chloride, in the most basic reaction with portlandite (phase of hydrated cement paste), decomposes into ammonia and water, and is very soluble in water $CaCl_2$. Calcium chloride dissociates into chloride ions and calcium ion, according to reaction (1):

$$Ca(OH)_2 + 2NH_4Cl \rightarrow Ca^{2+} + 2Cl^- + 2NH_3\uparrow + 2H_2O \quad (1)$$

Chloride ions and calcium ions diffuse in the pores of the concrete according to their concentration gradients [4, 10, 16]. NH_3 molecules escape from the pore solution and shift the reaction (1) to the right. This action contributes to the leaching of a larger amount of calcium ions from calcium solid phases, without the possibility of establishing equilibrium. In this way begins the decalcification process of the hardened cement paste, which results in the porosity increase [17]. According to Carde and François [18], the first dissolves portlandite, which leads to an increase in porosity of approximately 20% (CEM I), and thereby decreases in strength. In further stages decalcification of subsequent phases of hardened cement paste (aluminates, ettringite, Friedel's salts, silicates) occurs, and consequently their disappearance. These changes take place due to constantly lowering pH value of the concrete pore solution toward external surface. Based on data presented in Table 1, we can conclude which phases arise during this kind of corrosion process. The pH value of hardened cement paste is about 13 [1]. Table 1 also includes other phases that form in conditions of corrosion. They also interact with the hardened cement paste. For example, secondary ettringite crystallizes in the form of needles and occupies a large volume of the cement matrix, which causes its cracking. In the form of needles thaumasite also crystallizes, but this compound promotes the disintegration of the hydrated cement paste. Non-binding thaumasite crystallizes through dissolution of C-H and the most important binding phase – C-S-H gel [2, 5, 11, 14].

Materials and Methods

The most unfavorable situation was adopted in this study. Hardened cement paste, which represents the most susceptible corrosion component of concrete, was treated with ammonium and chloride ions as the most aggressive (to concrete) ions present in coke wastewater.

Hydrated cement paste specimens with w/c = 0.40 from Portland cement CEM I 42.5 R (series B) and slag cement CEM III/A 32.5 N-LH/HSR/NA (C series) were prepared. The chemical composition and phase composition of these cements are presented in Table 2 and in Table 3, respectively.

These cements were selected because Portland cement was widely used in the past to build wastewater treatment plants while slag cement is recommended currently for the construction of hydrotechnical structures and environmental issues. CEM III is produced in accordance with the principles of sustainable development and contains waste products from metallurgical processes.

Table 1. Calculated pH of water in equilibrium with the select solid phase at 20ºC [19, 20].

Phase	Portlandite	Calcium aluminate	Carboaluminate	Ettringite	Calcite	Thaumasite	Gypsum
pH	12,54	11,64	11,37	11,00	9,96	8,19	7,07

Table 2. The chemical composition of cements used for research (%).

Series	Cement	CaO	SiO_2	Al_3O_3	Fe_2O_3	SO_3	K_2O	Na_2O	MgO
B	CEM I 42,5 R	62,63	19,03	5,60	2,89	3,14	0,98	0,16	n. o.
C	CEM III/A 32.5 N-LH/HSR/NA	51,95	27,87	5,55	1,63	2,56	0,71	n. o.	4,21

Slag occupies about 50% of the weight of CEM III/A cement (Table 3).

Four cement paste specimens (250×250×60 mm) were cured for two weeks in moulds, and after demoulding were immersed in lime-saturated water for three months. Then one specimen of each kind of cement paste was immersed for 19 days in a saturated water solution of ammonium chloride (27% NH_4Cl) of pH=5. Nineteen days in these conditions is sufficient time to observe the changes of the microstructure, phase contents, porosity, and the distribution of chloride ions at a depth of about 11 mm. This was concluded on the basis of results obtained from a wider range of work performed in addition for 4 and 25 days [11].

These specimens subjected to aggression were designated as B-19 (made of cement CEM I 42.5 R) and C-19 (made of CEM III/A 32.5 N-LH/HSR/NA). The other two reference specimens were marked B-P (made of cement CEM I 42.5 R) and C-P (made of CEM III/A 32.5 N-LH/HSR/NA). B-P and C-P were protected against aggressive influences and stored in lime-water for four months.

After the removal from the ammonium chloride solution specimens were stored in a laboratory room at 20ºC±2ºC for two days.

Fractures were obtained and used for preliminary observations in order to determine the depth of location of the degradation front based on cement paste discoloration. Phases of hardened cement paste were observed and identified under the scanning electron microscope using the secondary (SE) electrons method. The capture of images was carried out with a ZEISS SUPRA 25 high-resolution scanning electron microscope with smartSEM and LEO 32 software. The images of microstructure were performed using backscattered electrons (BSE), with acceleration voltage = 20 kV, distance of the table from electron gun = 9 mm, and high vacuum (< $8{,}5\cdot10^{-5}$ mbar). Changes of porosity were estimated along the way of diffusion – from the specimen's surface into the core, using software for image analysis.

Table 3. The phase composition of cements used for research (%).

Series	Cement	C_3A	C_4AF	C_3S	Slag
B	CEM I 42.5 R	10	9	60	-
C	CEM III/A 32.5 N-LH/HSR/NA	5	4	30	50

Powdered hardened cement paste layers of thickness from the range of 0.5 to 2.0 mm were prepared using a grinding machine with a diamond head. Powdered layers were examined using X-ray diffractometry, which allowed us to determine the presence of crystalline phases. X-ray patterns were collected by the use of Cu-Kα radiation (45 kV, 35 mA). The HighScore software package of the PANalytical and PDF4+(2008) ICDD database was used for peaks identification.

Furthermore, analytical tests setting out the concentration of chloride ions depending on the distance from the specimens surface were prepared.

The scope of our research is shown in Fig. 1.

Results and Discussion

Numerical range describing each individual diffractogram of the powdered layer corresponds to the distance (in mm) from the specimen's external surface. The list of identified crystalline phases, indicated in Fig. 2, is shown in Table 4.

The analysis of results obtained from Portland cement specimen B-19 corroded for 19 days pointed out that portlandite disappeared at a depth of 0-5.0 mm; in this range it was not possible to detect its reflections. Belite, brownmillerite, and calcite were present along the entire length. In the surface layers of a range 0-3.5 mm we detected vaterite (7). Sulphate phases were present in the

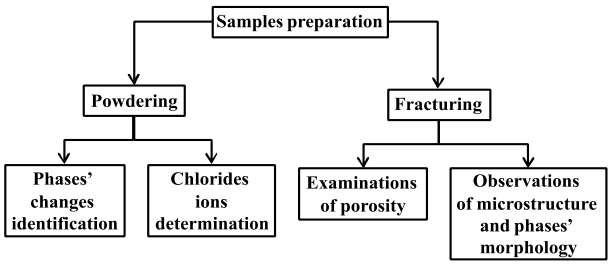

Fig. 1. Scheme of studies.

following distances from the surface: ettringite from 11.0 to 5.0 mm, thaumasite from 6.0 to 3.5 mm, and gypsum from 5.0 to 0.0 mm. Near gypsum, with the coordinates 0-4.5 mm from the sample's surface, we observed peaks of bassanite (8). It can also be assumed that Friedel's salt (2) was formed at the expense of carboaluminate (9).

There was no portlandite (1), or calcium aluminate (12) in the distance of 0 to 6.0 mm from the exterior surface, in layers taken from a corroded specimen made from slag cement after 19 days of immersion in NH_4Cl (C-19). Carboaluminate (9) was detected only in the layer of a range 8.0-10.0 mm. In all layers occurred calcite (6), and the intensity of its reflections were increasing, especially in the range of depth from 3.0 to 0 mm. Traces of vaterite also have been noted (7) in the area of calcite participation. Reflections of ackermanite (10) and belite (11) were found in all examined layers of the C-19 specimen from slag cement.

Contrary to specimen B-19 (from Portland cement), brownmillerite was not detected in the C-19 specimen from slag cement. However, in each layer of C-19 specimen were found the reflections of Friedel's salt (2). The reflections intensity of Friedel's salt was decreasing while content of gypsum (5) was significantly increasing – from the depth of 5.0 mm toward the external layer. Ettringite (3) was present to a depth of 1.5 mm. The presence of thaumasite (4) was stated firstly in layer from 5.0 to 6.0 mm. A small amount of the solid solution of ettringite-thaumasite was contained in the layer located at a distance 2.0-3.0 mm from the surface. At a distance of 0.5-1.0 mm from the surface we detected only thaumasite.

To confirm the presence of phases detected by the diffractometry method, observations of fractures under the scanning electron microscope (using scattered secondary electrons) were made. In this examination we also observed phases that during X-ray identification were not possible to detect due to their small volume. In other cases, the high content of amorphous phases reduced the likelihood of their detection. For example, on the surface of corroded slag cement specimen C-19 appeared anhydrite in the form of columnar crystals (Fig. 3a).

The damaged areas of both specimens, B-19 and C-19, revealed high porous microstructure of hardened cement paste. The voids in the microstructure showed (Fig. 3b), arisen probably through dissolution of cement grains by the action of aggressive NH_4Cl water solution.

Fig. 4 shows an exemplary picture taken in the area of micro-section under scanning electron microscope using

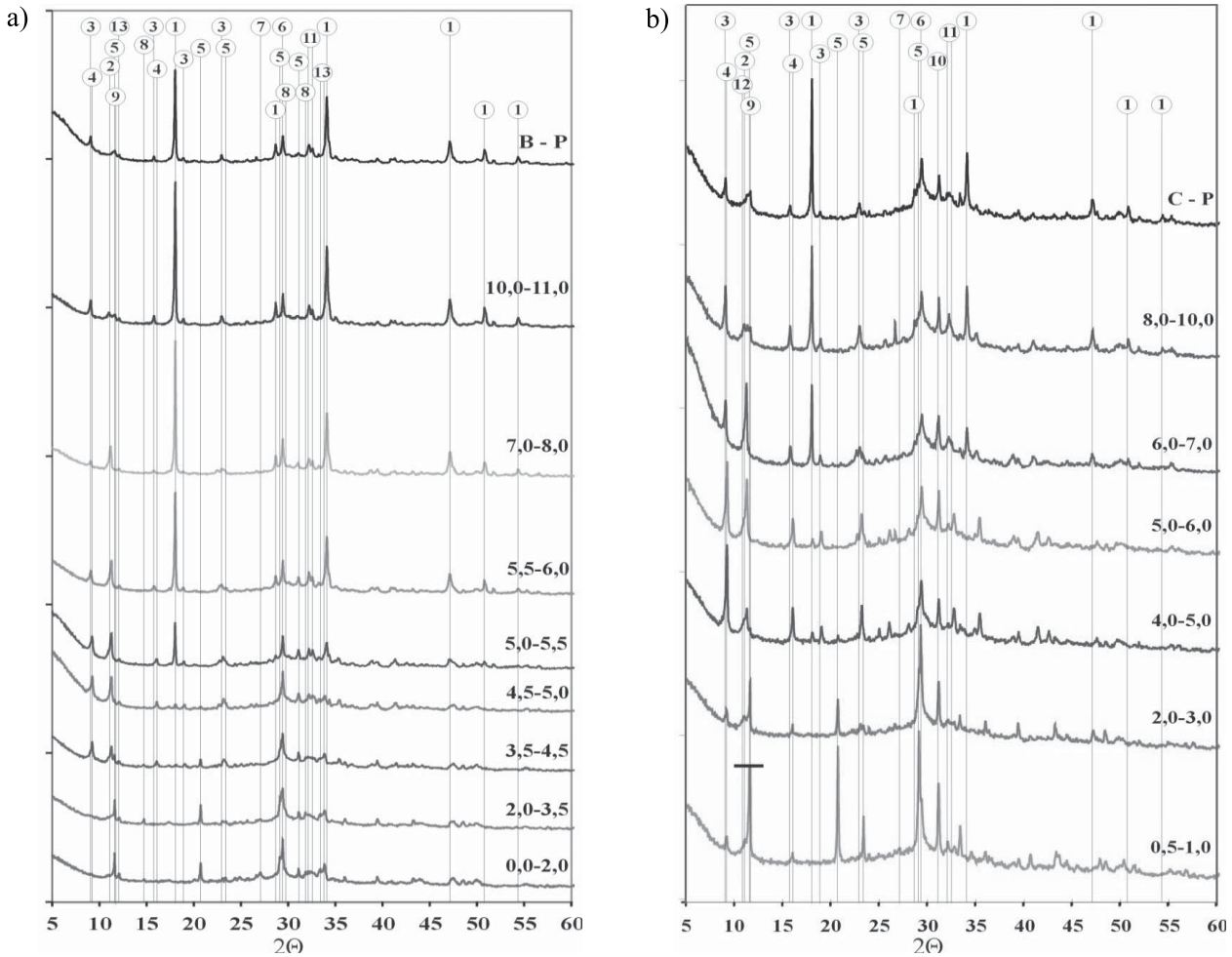

Fig. 2. Diffraction patterns of material taken from samples of hardened cement paste: a) B-19 and B-P (CEM I 42.5R), b) C-19 and C-P (CEM III/A 32.5 N-LH/HSR/NA).

Table 4. List of identified hardened cement paste phases.

No.	Phase	Origin of the phase	Stoichiometric formula in cement chemistry	Stoichiometric formula
1.	Portlandite	initial phase	CH	$Ca(OH)_2$
2.	Friedel's salt	presence of chlorides	$C_3A{\cdot}CaCl_2{\cdot}H_{10}$	$Ca_4Al_2O_6Cl_2{\cdot}10H_2O$
3.	Ettringite, AFt	initial phase, and in large quantities; effect of sulphate and acid corrosion	$C_6A\bar{S}_3{\cdot}H_{32}$	$Ca_6Al_2(SO_4)_3(OH)_{12}{\cdot}26H_2O$
4.	Thaumasite	sulphate or acid corrosion	$C_3S\hat{C}\bar{S}{\cdot}H_{15}$	$Ca_3Si(CO_3)(SO_4)(OH)_6{\cdot}12H_2O$
5.	Gypsum	sulphate or acid corrosion	$C\bar{S}H_2$	$Ca(SO_4)(H_2O)_2$
6.	Calcite	initial phase in trace amounts or effect of carbonation of hardened cement paste	$C\hat{C}$	$CaCO_3$
7.	Vaterite	effect of carbonation of hardened cement paste	$C\hat{C}$	$CaCO_3$
8.	Bassanite	hemihydrate, the product of dehydration of gypsum	$C\bar{S}H_{0,5}$	$Ca(SO_4)(H_2O)_{0,5}$
9.	Carboaluminate	initial phase in trace amounts or effect of carbonation of hardened cement paste	$C_3A{\cdot}C\hat{C}{\cdot}H_{11}$	$Ca_4Al_2O_6CO_3{\cdot}11H_2O$
10.	Ackermanite	initial slag phase	C_2MS_2	$Ca_2Mg(Si_2O_7)$
11.	Belite	initial phase	C_2S	Ca_2SiO_4
12.	Calcium aluminate	initial phase	$C_4A{\cdot}H_{13}$	$Ca_4Al_2O_7{\cdot}13H_2O$
13.	Brownmillerite	initial phase	C_4AF	Ca_2FeAlO_5

backscattered electron detection (SEM-BSE). This image has been selected from the series of shots made one after another, along the way of diffusion of aggressive ions – from the surface to the core. Areas of pores on each image were summed. Each sum was divided by the whole area of a given image. Subsequently, porosity distribution was obtained (relatively to the center of a given image and the depth from the specimen's surface), which is presented in the collective Figs. 5a and 6a.

Percentage of the pores in comparative specimens was 5.2 and 5.5 in B-P and C-P, respectively. The aggressive action of NH_4Cl caused increases in porosity in the direction of external zones in both kinds of hardened cement paste specimens. The porosity of corroded specimen made of Portland cement B-19, in relation to the corroded slag cement specimen C-19, was slightly lower. In the case of corroded Portland cement hydrated paste B-19 from 2 mm in the direction of external surface, porosity was decreasing. This phenomenon can be explained by filling the earlier-formed voids with calcium carbonate and gypsum. This indicated tendency was not observed in the case of corroded slag cement hardened paste C-19. So it can be deduced that even large amounts of corrosion products did not fulfill the discontinuities.

The content of chloride ions along the way of diffusion in the hardened cement paste is shown in Figs. 5b and 6b.

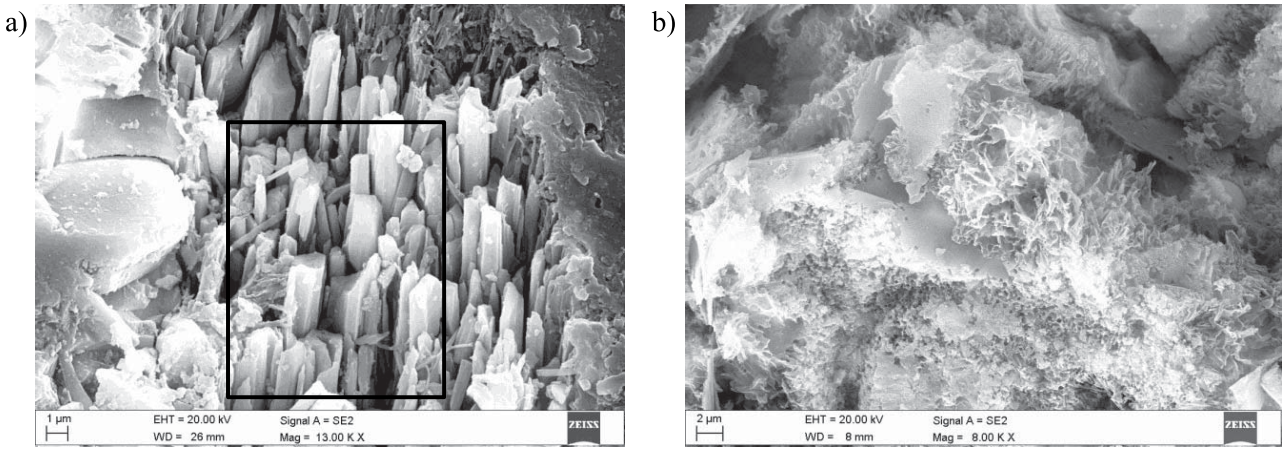

Fig. 3. Microstructure of corroded slag cement-hardened paste in C-19 specimen: a) anhydrite at a distance of 20 µm from the external layer, b) image at a distance of 1000 µm from the external layer.

Chloride ion concentrations in specimens B-P and C-P immersed only in water solution of calcium hydroxide were at levels 0g/10g of the powdered hydrated cement paste. Curves of chloride ion concentrations consist of rising and falling parts. Chloride concentration in the surface layer, contrary to expectations, was not the largest, which can be explained by the boundary disorders resulting from the significant damage of material [11]. The distribution of chloride concentrations in both cases is very similar. These graphs represent both the concentration derived from penetration of Cl^- ions from the external environment as well as from their release, a result of dissolution of the secondarily formed chloride phases, among others Friedel's salt. This is particularly noticeable in the case of corroded slag cement specimen C-19 (Fig. 6b). The increase in the content of chloride ions from both sides is covered at a depth of about 2.7 mm in the case of specimen B-19. Therefore, the concentrations of chloride ions in the case of Portland cement (B-19) was slightly higher than in corroded slag cement hardened paste C-19.

The comparison of examination results of corroded specimens indicates that the content of crystalline phases is fairly similar in these two cases. Ackermanite (A) was not detected in specimen B-19 because it is a slag phase. Reflections of brownmillerite (B) – initial phase of the hardened paste and reflections of vaterite (V) – an unstable polymorph of calcium carbonate, were not identified in the case of corroded slag cement paste C-19. A huge amount of gypsum was crystallized in corroded slag cement paste C-19. It should seem that it probably helped to reduce porosity in the C-19 specimen to a greater extent in comparison to corroded specimens made of Portland cement (B-19). However, the results were opposite. If so, slag cement hardened paste (from CEM III) did not make as large a barrier of defense as hardened Portland cement paste (from CEM I).

It is generally known that the higher the porosity of hardened cement paste, the faster aggressive substances penetrate the concrete. Because of this, characteristic points on graphs of specimen C-19 are moved deeper than in specimen B-19. These inferior protective properties of hardened slag cement CEM III can be explained by too small portlandite content in untreated hardened paste. This essentially determined the duration of the first stage of the decalcification process. Calcium hydroxide sustains the durability of other calcium hydrates. However, when pH decreases, $Ca(OH)_2$ can contribute to the formation of thaumasite – one of the most dangerous products of corrosion of hardened cement paste. Thaumasite was identified in much larger amounts in corroded slag cement hardened paste (specimen C-19) than in corroded Portland cement hardened paste (specimen B-19).

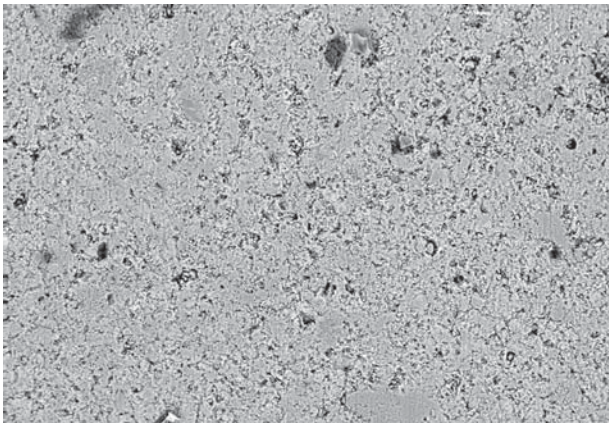

Fig. 4. SEM-BSE microscopic images of the external area of B-19 sample of paste from Portland cement (CEM I 42.5 R), at 1781.4-2691.4 μm depth.

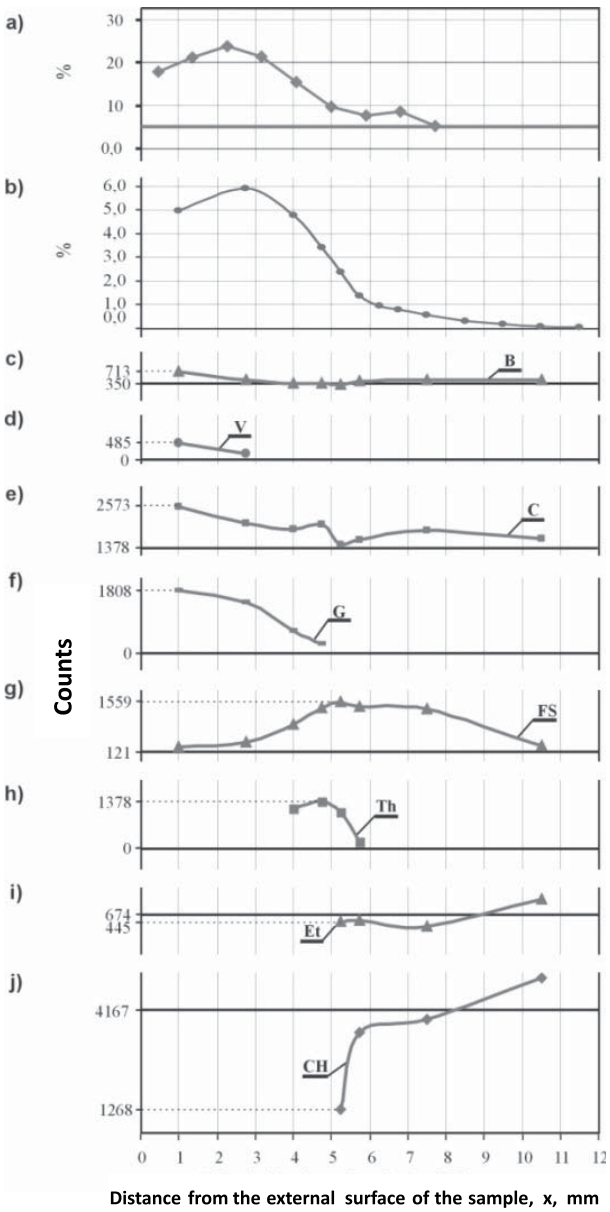

Fig. 5. The changes of content in specimen B-19 as well as B-P (horizontal lines) related to a) porosity, b) concentration of chloride ions and phase content: c) brownmillerite, d) vaterite, e) calcite, f) gypsum, g) Friedel's salt, h) thaumasite, i) ettringite, and j) portlandite.

Conclusions

The wastewater from coke plants causes damage to facilities made of concrete. From the point of view of cement paste destruction, the most aggressive ions contained in this sewage are chlorides and ammonium. While the concrete gets unstable, it does not meet the protective properties for steel reinforcement. It leads to the destruction of the sewage tank walls as porosity and permeability increase but strength decreases. Leakage into groundwater is inevitable.

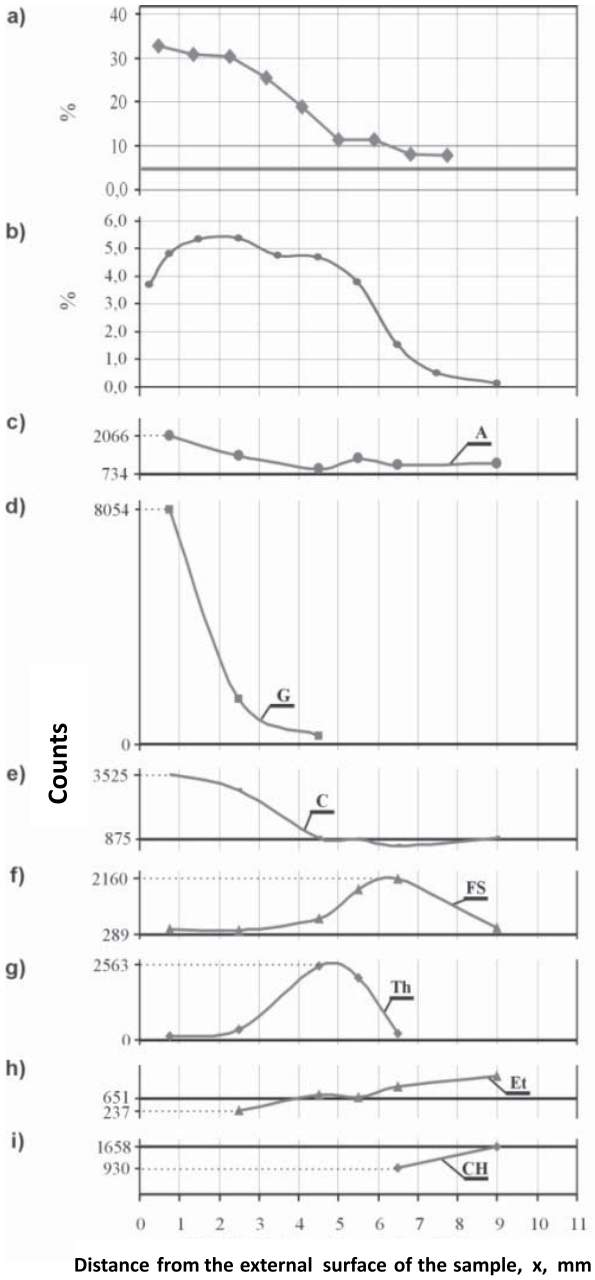

Fig. 6. The changes of content in speci-men C-19 as well as C-P (horizontal lines) related to a) porosity, b) concentra-tion of chloride ions and phase content: c) ackermanite, d) gypsum, e) calcite, f) Friedel's salt, g) thaumasite, h) ettringite, and i) port-landite.

The presented experimental research of corrosion of hardened pastes made of two different cements used for the construction of sewage treatment plant tanks in the past and currently recommended, after 19 days of action of a saturated aqueous solution of ammonium chloride, revealed many significant changes determining the durability of these materials.

Hardened Portland cement paste in comparison with the hardened slag cement paste posed greater resistance to aggressive substances in the sense of reacting and penetrating. Undoubtedly, the higher amount of portlandite in composition of hardened Portland cement paste contributed to this fact.

The slag cement hardened paste (specimen C-19) proved to have worse protective and durable properties. Larger porosity and greater amount of dangerous crystalline products, primarily thaumasite and gypsum, formed in the case of the C-19 specimen. And in the case of the C-19 specimen much more Friedel's salt crystallized. The dissolution of this phase caused an increase in free chloride ions content in the pore solution, under lowering pH value. Results indicated that the most important factors determining the rate of cement paste corrosion are porosity and susceptibility to reaction with the components of wastewater. Therefore, the composition of cements produced in accordance with the principles of sustainable development – containing waste products, for instance from metallurgical processes – should be selected according to specific features of the environment, which will contact the concrete made of this cement. Unfortunately, for now blast furnace slag cement (CEM III) appears to be less resistant to corrosion under select components of coke sewage.

Acknowledgements

This work was partially supported by project POIG.01.01.02-10-106/09-00 of the Operational Program Innovation Economy.

References

1. KURDOWSKI W. The Chemistry of Cement and Concrete. Polski Cement, Kraków 2010. Wydawnictwo Naukowe PWN, Warszawa **2010** [in Polish].
2. KURDOWSKI W. C-S-H phase, state of the art. Part 2. Cement Wapno Beton, **5**, 258, **2008**.
3. JAŚNIOK T. Potentiodynamic polarization test in reinforced concrete during passivation and corrosion of steel, caused by carbonation of concrete. Ochr. Przed Koroz., **1**, (3-9), **2009** [in Polish].
4. ČERNÝ R., ROVNANÍKOVÁ P. Transport processes in concrete. Spon - Press London and New York, **2002**.
5. SŁOMKA-SŁUPIK B., ZYBURA A. Corrosion of Portland cement pastes produced from CEM I 42,5R and CEM I 42,5R-HSR/NA in ammonium chloride solution. Cement Wapno Beton, **3**, 144, **2012**.
6. JANOSZ-RAJCZYK M. Biological methods of nitrogen removing from selected wastewater. Series: Monographs,

nr 102. Częstochowa University of Technology Publishing. Częstochowa **2004** [in Polish].
7. MINHALMA M., PINHO M.N. Development of nanofiltration/steam stripping sequence for coke plant wastewater treatment. Desalination **149**, 95, **2002**.
8. JAŚNIOK T., JAŚNIOK M. The variability of the rate of corrosion of reinforcement in concrete at constant temperature and humidity conditions. Ochr. Przed Koroz., **55** (6), 282, **2012** [in Polish].
9. SANDBERG P. Studies of chloride binding in concrete exposed in a marine environment. Cement and Concrete Research **29**, 473, **1999**.
10. SUGIYAMA T., RITTHICHAUY W., TSUJI Y. Simultaneous transport of chloride and calcium ions in hydrated cement systems. Journal of Advanced Concrete Technology – Japan Concrete Institute, **1** (2), 127, **2003**.
11. SŁOMKA-SŁUPIK B., ZYBURA A. Chloride ions diffusion in hydrated cement paste immersed in saturated NH_4Cl. Cement Wapno Beton, **5**, 232, **2009**.
12. GLASS G.K., BUENFELD N.R. The influence of chloride binding on the chloride induced corrosion risk in reinforced concrete. Corrosion Science, **42**, 329, **2000**.
13. ZYBURA A. Analysis of chloride migration in concrete based on multicomponent medium theory. Archives of Civil Engineering **53** (1), 131, **2007**.
14. BENSTED J. Thaumasite. Part 1: The route to current understanding. Cement Wapno Beton, **4**, 165, **2007**.
15. MAŁOLEPSZY J., MRÓZ R. Conditions of thaumasite formation. Cement Wapno Beton, **2**, 93, **2006**.
16. JAŚNIOK T., SŁOMKA-SŁUPIK B., ZYBURA A. The concrete reinforcement chloride corrosion, immediately after its initiation. Cement Wapno Beton, 3, 158, **2014**.
17. SŁOMKA-SŁUPIK B., ZYBURA A. The coking wastewater action to concrete of environmental protection facilities. XV Scientific-Technical Conference: Structures Durability and Corrosion Protection KONTRA '2006, Warszawa-Zakopane, 25-27 May 2006. Published in: Ochr. Przed Koroz., (141-148) **5s/A/2006** [in Polish].
18. CARDE C., FRANÇOIS R. Effect of the leaching of calcium hydroxide from cement paste on mechanical and physical properties. Cement and Concrete Research **27** (4), 539, **1997**.
19. DAMIDOT D. Improvement of calcium aluminate cement resistance to sulfate and carbonate attacks by silica addition: thermodynamic approach. Proceedings of the International Colloquium held at Mogilany 16-17 Nov. 1994: Corrosion of cement paste – edited by W. Kurdowski. Akapit, Kraków **1995**.
20. KÖHLER S., HEINZ D., URBONAS L. Effect of ettringite on thaumasite formation. Cement and Concrete Research **36**, 697, **2006**.